

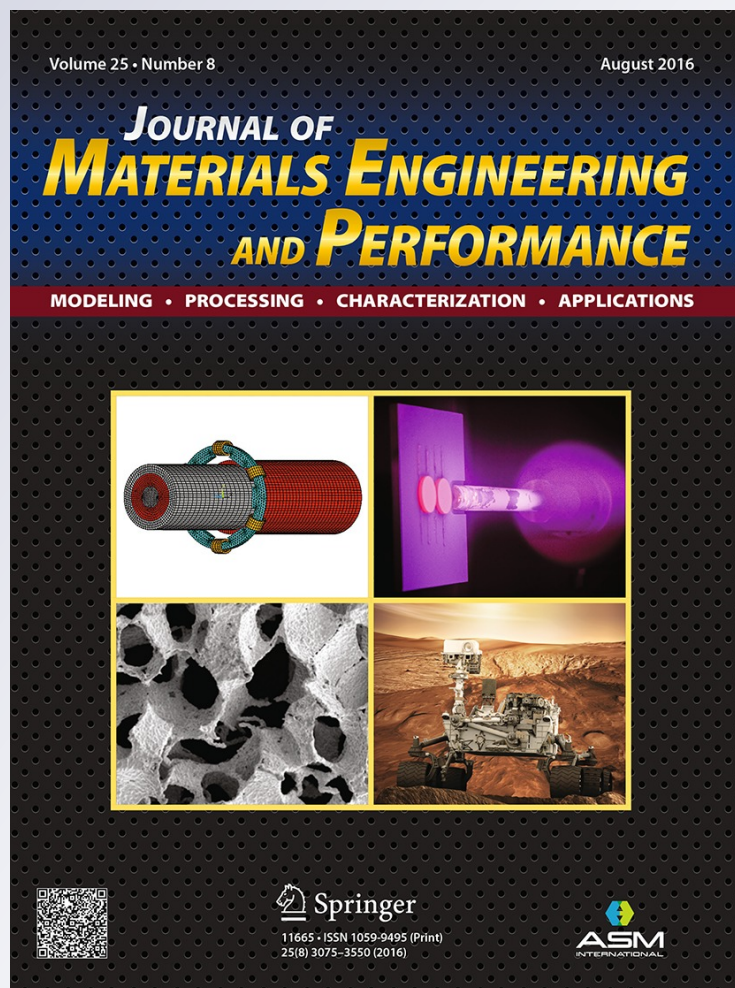
Observation of Pseudopartial Grain Boundary Wetting in the NdFeB-Based Alloy

**B. B. Straumal, A. A. Mazilkin,
S. G. Protasova, G. Schütz,
A. B. Straumal & B. Baretzky**

Journal of Materials Engineering and Performance

ISSN 1059-9495
Volume 25
Number 8

J. of Materi Eng and Perform (2016)
25:3303-3309
DOI 10.1007/s11665-015-1872-8



Your article is protected by copyright and all rights are held exclusively by ASM International. This e-offprint is for personal use only and shall not be self-archived in electronic repositories. If you wish to self-archive your article, please use the accepted manuscript version for posting on your own website. You may further deposit the accepted manuscript version in any repository, provided it is only made publicly available 12 months after official publication or later and provided acknowledgement is given to the original source of publication and a link is inserted to the published article on Springer's website. The link must be accompanied by the following text: "The final publication is available at link.springer.com".

Observation of Pseudopartial Grain Boundary Wetting in the NdFeB-Based Alloy

B.B. Straumal, A.A. Mazilkin, S.G. Protasova, G. Schütz, A.B. Straumal, and B. Baretzky

(Submitted November 14, 2015; published online March 18, 2016)

The NdFeB-based alloys were invented in 1980s and remain the best-known hard magnetic alloys. In order to reach the optimum magnetic properties, the grains of hard magnetic Nd₂Fe₁₄B phase have to be isolated from one another by the (possibly thin) layers of a non-ferromagnetic Nd-rich phase. In this work, we observe that the few-nanometer-thin layers of the Nd-rich phase appear between Nd₂Fe₁₄B grains due to the pseudopartial grain boundary (GB) wetting. Namely, some Nd₂Fe₁₄B/Nd₂Fe₁₄B GBs are not completely wetted by the Nd-rich melt and have the high contact angle with the liquid phase and, nevertheless, contain the 2–4-nm-thin uniform Nd-rich layer.

Keywords grain boundaries, hard magnetic materials, phase transitions, wetting

1. Introduction

The developments of last decade show that the properties of fine-grained and nanograined materials are critically controlled by the behavior of grain boundaries (GBs) and triple junctions (TJs) (Ref 1, 2). Moreover, the most advanced experimental methods like high-resolution electron microscopy (HREM) and atom probe microscopy allowed observing that GBs and TJs are frequently not atomically thin and smooth but contain the few-nm-thick layers or so-called complexions (Ref 3–15). These layers can appear in equilibrium, non-equilibrium

This article is an invited submission to JMEP selected from presentations at the Symposium “Wetting and High-Temperature Capillarity,” belonging to the Topic “Joining and Interfaces” at the European Congress and Exhibition on Advanced Materials and Processes (EUROMAT 2015), held during September 20–24, 2015, in Warsaw, Poland, and has been expanded from the original presentation.

B.B. Straumal and **A.B. Straumal**, Institute of Solid State Physics, Russian Academy of Sciences, Ac. Ossipyan str. 2, 142432 Chernogolovka, Moscow District, Russia; **Karlsruher Institut für Technologie**, Institut für Nanotechnologie, Hermann-von-Helmholtz-Platz 1, 76344 Eggenstein-Leopoldshafen, Germany; and **National University of Science and Technology (MISIS)**, Leninsky prosp. 4, 119991 Moscow, Russia; **A.A. Mazilkin**, Institute of Solid State Physics, Russian Academy of Sciences, Ac. Ossipyan str. 2, 142432 Chernogolovka, Moscow District, Russia and **Karlsruher Institut für Technologie**, Institut für Nanotechnologie, Hermann-von-Helmholtz-Platz 1, 76344 Eggenstein-Leopoldshafen, Germany; **S.G. Protasova**, Institute of Solid State Physics, Russian Academy of Sciences, Ac. Ossipyan str. 2, 142432 Chernogolovka, Moscow District, Russia and **Max-Planck-Institute for Intelligent Systems**, Heisenbergstr. 3, 70569 Stuttgart, Germany; **G. Schütz**, **Max-Planck-Institute for Intelligent Systems**, Heisenbergstr. 3, 70569 Stuttgart, Germany; and **B. Baretzky**, **Karlsruher Institut für Technologie**, Institut für Nanotechnologie, Hermann-von-Helmholtz-Platz 1, 76344 Eggenstein-Leopoldshafen, Germany. Contact e-mail: straumal@issp.ac.ru.

(transient), or steady-state structures (Ref 4–22). Most interesting, from our point of view, is the phenomenon of the so-called pseudopartial (or pseudo-incomplete) GB wetting (marked as PPW in the generic phase diagram in Fig. 1g proposed in Ref 23) (Ref 24–26). It is an intermediate between complete (CW, Fig. 1g) and partial (PW, Fig. 1g) GB wetting.

Let us consider a partially melted two- or multicomponent polycrystal. It corresponds to the condition that temperature is between the solidus temperature T_S and the liquidus temperature T_L . Consider the droplet of a liquid phase on the surface of a solid phase or between two solid grains. Usually, one distinguishes partial and complete wetting of surfaces or interfaces. If the liquid droplet partially wets a solid surface (Fig. 1a), then $\sigma_{sg} - \sigma_{sl} = \sigma_{lg} \cos \theta$, where σ_{sg} is the free energy of solid/gas interface, σ_{sl} is the free energy of solid/liquid interface, σ_{lg} is that of liquid/gas interface, and θ is the contact angle. If the liquid droplet partially wets the boundary between two solid grains (Fig. 1b), then $\sigma_{gb} = 2\sigma_{sl} \cos \theta$, where σ_{gb} is the free energy of a grain boundary (GB). The free surface or GB which is not covered by the liquid droplets remains dry and contains only the adsorbed atoms with coverage below one monolayer. In this case, the GB can exist in the equilibrium contact with the liquid phase. In the case of complete wetting (Fig. 1c, d) $\sigma_{sg} > \sigma_{lg} + \sigma_{sl}$ or $\sigma_{gb} > 2\sigma_{sl}$, the contact angle is zero, and liquid spreads over the free surface or between grains. In this case, the GB separating the grains is completely substituted by the liquid phase.

The transition from incomplete to complete (partial) GB wetting proceeds at a certain T_w if the energy of two solid-liquid interfaces $2\sigma_{SL}$ becomes lower than the GB energy $\sigma_{GB} > 2\sigma_{SL}$. Cahn (Ref 27) and Ebner and Saam (Ref 28) first showed that the (reversible) transition from incomplete to complete wetting can proceed with increasing temperature and that it is a true surface phase transformation. The GB wetting temperatures, T_w , depend both on GB energy and solid-liquid interfacial energy which, in turn, depend on the crystallography of these interfaces (Ref 29–32). The transition from incomplete to complete GB wetting starts at a certain minimum temperature T_{wmin} which corresponds to the combination of maximum σ_{GB} and minimum σ_{SL} . The transition from incomplete to complete GB wetting finishes at a maximum temperature T_{wmax} which corresponds to the combination of minimum σ_{GB} and

maximum σ_{SL} . The fraction of completely wetted GBs increases from 0 to 100% as the temperature increases from T_{wmin} to T_{wmax} . (Ref 33–39). As a result, the new tie lines appear in the S + L area of a phase diagram at T_{wmin} and T_{wmax} (Ref 33–39).

In the case of complete wetting (Fig. 1c, d) $\sigma_{sg} > \sigma_{lg} + \sigma_{sl}$ or $\sigma_{gb} > 2\sigma_{sl}$, the contact angle is zero, and liquid spreads over the free surface or between grains. What happens, if the amount of liquid is small and surface (or GB) area is large? In this case, the liquid spreads until both solid grains or solid and gas begin to interact with each other through the liquid layer. The liquid forms a “pancake” with a thickness e_s of about 2-5 nm (Ref 8, 40):

$$e_s = (A/4\pi S)^{1/2}, \quad (\text{Eq 1})$$

where $S = \sigma_{sg} - \sigma_{sl} - \sigma_{lg}$ is the spreading coefficient on a strictly “dry” solid and A is the Hamaker constant (Ref 40). In case of complete wetting, $A > 0$ and $S > 0$ (Ref 40). Such “pancake” on the free surface or between the grains is formed by the deficit of a wetting phase, i.e., in the $\alpha + L$ two-phase area of a phase diagram, but very close to the solidus line.

In the majority of cases, the direct transition occurs from partial wetting into complete wetting, for example by increasing temperature (Ref 32, 36, 41) or decreasing pressure (Ref 42). However, in some cases the state of pseudopartial wetting occurs (PPW in Fig. 1g) between partial and complete wetting. In this case, the contact angle $\theta > 0$, and the liquid droplet does not spread over the substrate, but the thin (few nm) precursor film exists around the droplet and separates substrate and gas (Fig. 1e). Such precursor film is very similar for the liquid “pancake” which forms in case of complete wetting and deficit of the liquid phase. This case is called pseudopartial wetting, and it is possible when $A < 0$ and $S > 0$ (Ref 40). In case of pseudopartial wetting, the precursor exists together with liquid droplets, and in case of complete wetting the droplets disappear forming the “pancake.”

The sequence of discontinuous PW \leftrightarrow PPW and continuous PPW \leftrightarrow CW has been observed for the first time in the alkanes/water mixture (Ref 43). The critical end point (CEP in Fig. 1f) was observed in a mixture of pentane and hexane which was deposited on an aqueous solution of glucose (Ref 23). The first direct measurement of the contact angle in the intermediate wetting state (pseudopartial wetting) was performed in the sequential-wetting scenario of hexane on salt brine (Ref 43). Later, the formation of Pb, Bi, and binary Pb-Bi precursors surrounding liquid or solidified droplets has been observed on

the surface of solid copper (Ref 44). The pseudopartial wetting has been observed recently also for GBs (Fig. 1f) in Al-Zn (Ref 24, 25) and W-C-Co (Ref 26) systems. The 2-4-nm-thin layers of the soft Zn-rich phase between Al grains lead to the superductility of the ultrafine-grained Al-Zn alloys obtained by the high-pressure torsion (Ref 20, 21, 45, 46). The analysis of existing literature permitted us to suppose that the pseudopartial GB wetting exists also in the Fe-Nd-B-based hard magnetic alloys (Ref 47). The goal of this work is to experimentally prove this hypothesis.

2. Experimental

The Nd-Fe-B-based liquid-phase sintered alloy was purchased from the company Vacuumschmelze GmbH (Germany): it contained 66.5 wt.% Fe, 22.1 wt.% Nd, 9.4 wt.% Dy, 1.0 wt.% Co, 0.8 wt.% B, and 0.2 wt.% Cu. The as-delivered samples were cut into $2 \times 4 \times 6$ mm specimens (for the investigations of GB wetting behavior) and $3 \times 3 \times 3$ mm specimens (for magnetic measurements). The samples were sealed into evacuated silica ampoules with a residual pressure of approximately 4×10^{-4} Pa at room temperature. They were annealed at 900 °C for 2 h and then quenched in water. The accuracy of the annealing temperature was ± 1 °C. Transmission electron microscopy (TEM, HRTEM, STEM, EDXS) studies were carried out on the on the TECNAI instrument. X-ray diffraction (XRD) data were obtained on a Siemens diffractometer (Co K α radiation). TEM lamellas were prepared on the STRATA dual-beam facility. The magnetic properties were measured on a superconducting quantum interference device SQUID (Quantum Design MPMS-7 and MPMS-XL).

3. Results

In Fig. 3a, the STEM micrograph of a triple joint between is shown. The chemical composition of these three grains measured by the EDXS in TEM corresponds to that of Nd₂Fe₁₄B hard magnetic phase. The triple joint shown in Fig. 3a is filled by the Nd-rich phase which was liquid during the liquid-phase sintering and annealing at 900 °C (Ref 48–50). Fig. 3d, e, and f shows the Fe and Nd concentration profiles across all three Nd₂Fe₁₄B/Nd₂Fe₁₄B GBs in the locations C, B, and A (Fig. 3a), respectively. The first two profiles do not contain any Fe and/or Nd maxima or minima. It means that the respective GBs C

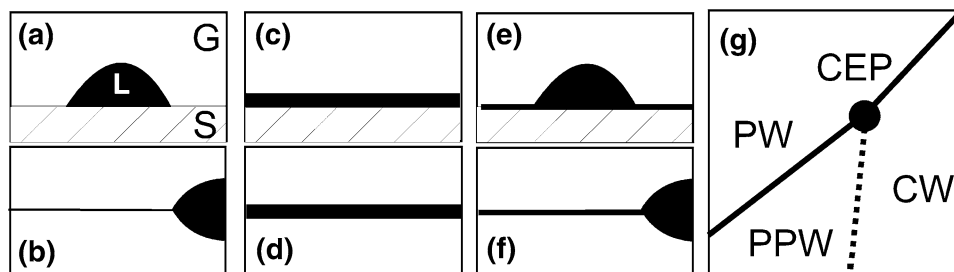


Fig. 1 The schemes for the wetting of free surfaces and GBs. (a) partial surface wetting, L – liquid phase, S – solid phase, G – gas phase; (b) partial GB wetting; (c) complete surface wetting; (d) complete GB wetting; (e) pseudopartial surface wetting; (f) pseudopartial GB wetting; (g) generic wetting phase diagram [23], PW – partial wetting, CW – complete wetting, PPW – pseudopartial wetting, CEP – critical end point, thick lines mark the discontinuous (first order) wetting transition, thin line mark the continuous (second order) wetting transition

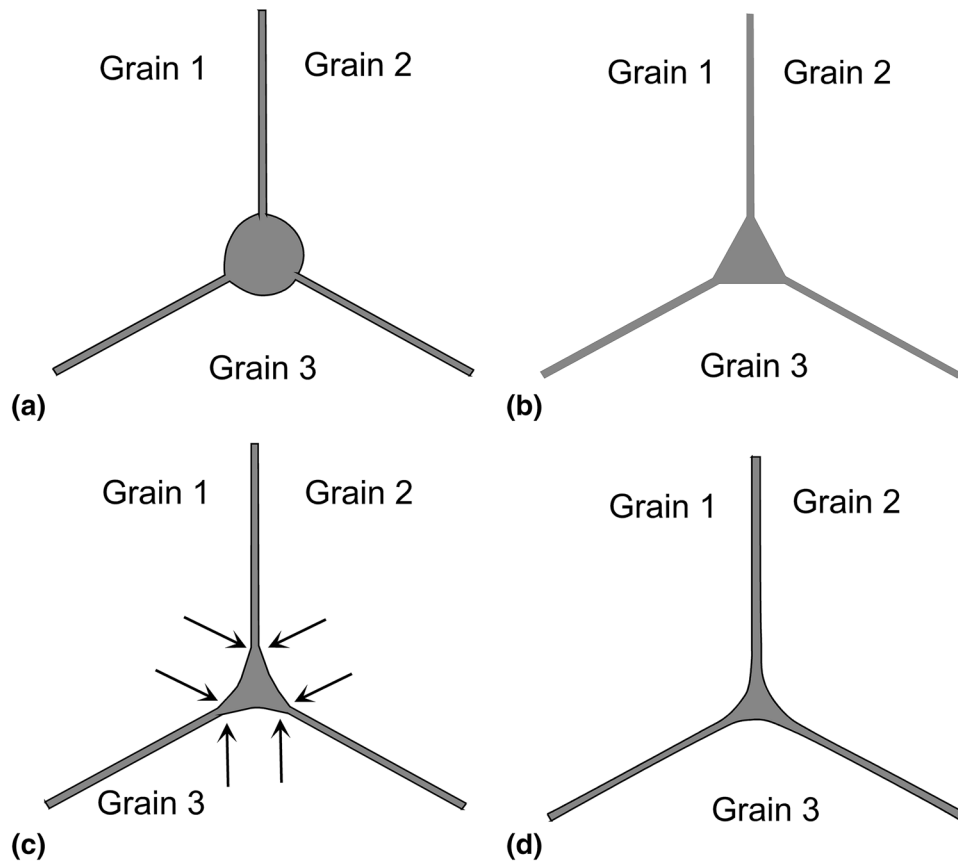


Fig. 2 Different configurations of liquid phase in the GB triple junction and thin quasi-liquid thin layers in the GB. (a) Pseudopartial GB wetting, $\theta > 60^\circ$. (b) Pseudopartial GB wetting, $\theta = 60^\circ$. (c) Pseudopartial GB wetting, $\theta < 60^\circ$. The contact points between liquid phase in TJ and quasi-liquid layers in the GB are shown by arrows. (d) Complete GB wetting, $\theta = 0^\circ$

and B remain “dry” and are not enriched (depleted) by the Fe and/or Nd. The GBs C and B have the non-zero contact angle with Nd-rich phase in the TJ. In other words, the GBs C and B are incompletely (partially) wetted by the Nd-rich melt. This situation corresponds to the scheme shown in Fig. 1b.

The GB A is different. The concentration profile in Fig. 3f shows that the GB A is enriched by Nd and depleted by Fe. The thickness of the Nd maximum and Fe minimum is about 5 nm. The uniformly thin light-gray layer of an Nd-rich phase in GB A is clearly visible also in Fig. 3a. Figure 3b shows the conventional TEM micrograph of this GB, and Fig. 3c contains the micrograph of the same GB with a thin layer of an Nd-rich phase. Both TEM and HREM also witness that the Nd-rich GB layer is uniformly thin and has a thickness of about 5 nm. The GB A, similar to the GBs C and B, also has the non-zero contact angle with Nd-rich phase in the TJ. Since GB A is not “dry” and contains the thin Nd-rich layer, this situation corresponds to the scheme shown in Fig. 1f and 2c. In other words, the GB C is pseudo-incompletely (or pseudopartially) wetted by the Nd-rich melt.

4. Discussion

The NdFeB-based alloys were invented in 1980s. They remain the best-known hard magnetic alloys with the highest magnetic energy product HB (B being the flux density and H

being the field strength). In order to reach the optimum magnetic properties, the $\text{Nd}_2\text{Fe}_{14}\text{B}$ grains have to be isolated from one another by the layers of a non-ferromagnetic phase. In most cases, it is the Nd-rich phase. It forms during the liquid-phase sintering as a liquid layer between $\text{Nd}_2\text{Fe}_{14}\text{B}$ grains. It has been demonstrated rather early (Ref 51) that the thickness of these layers needed for effective magnetic isolation between $\text{Nd}_2\text{Fe}_{14}\text{B}$ grains is only few nanometers (Ref 52). If the total amount of the Nd-rich phase is too high, it decreases the saturation magnetization of an alloy as a whole. Therefore, the amount of the Nd-rich phase has to be kept as low as possible, namely at the level which is minimally needed for the effective magnetic isolation between grains of the hard magnetic $\text{Nd}_2\text{Fe}_{14}\text{B}$ phase.

The most broadly used technology for the production of NdFeB-based hard magnetic alloys is the liquid-phase sintering of a rather coarse-grained (10–20 μm) $\text{Nd}_2\text{Fe}_{14}\text{B}$ powders. The liquid-phase sintering usually proceeds close to 1100 $^\circ\text{C}$ (Ref 53, 54). The contact angles between melt and the $\text{Nd}_2\text{Fe}_{14}\text{B}/\text{Nd}_2\text{Fe}_{14}\text{B}$ GBs were experimentally measured in the temperature interval between 700 and 1100 $^\circ\text{C}$ (Ref 55). Even at the highest studied temperature of 1100 $^\circ\text{C}$, the portion of completely wetted $\text{Nd}_2\text{Fe}_{14}\text{B}/\text{Nd}_2\text{Fe}_{14}\text{B}$ GBs was slightly above 80%. It quickly decreased with decreasing temperature, and at 700 $^\circ\text{C}$ GBs it was only around 10%. These results concern the “pure” three-component Nd-Fe-B alloys. The micrographs published in the literature permitted us to estimate the amount of completely wetted $\text{Nd}_2\text{Fe}_{14}\text{B}/\text{Nd}_2\text{Fe}_{14}\text{B}$ GBs in the alloys

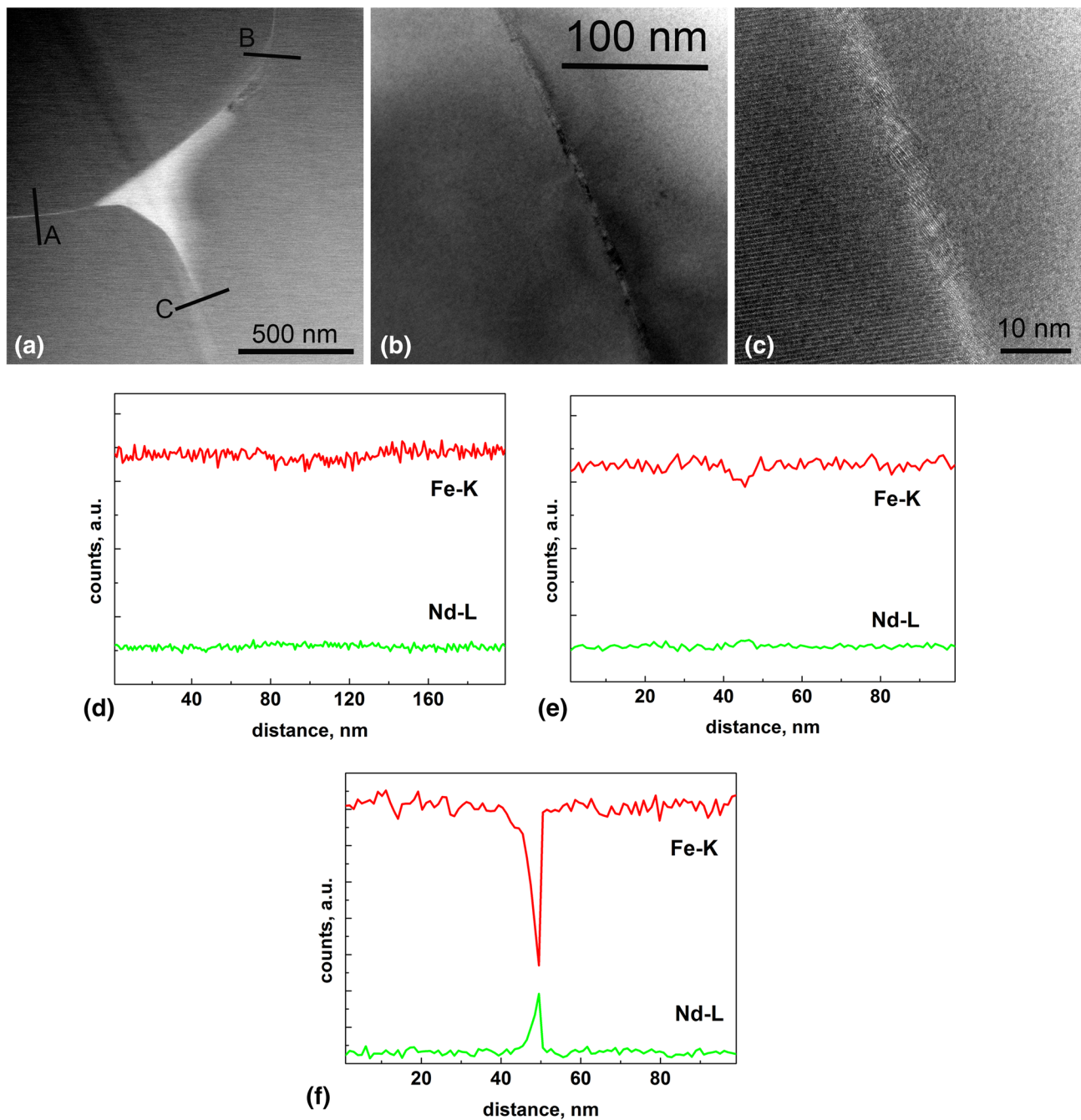


Fig. 3 (a) STEM micrograph of a triple joint between three Nd₂Fe₁₄B grains filled by the Nd-rich phase. The positions of concentration profiles are shown (A, B and C). (b) Conventional TEM micrograph of a GB A containing the uniformly thin layer of a Nd-rich phase. (c) HREM micrograph of the same GB with a thin layer of a Nd-rich phase. (d, e, f) Fe and Nd concentration profiles in the locations C, B and A, respectively

containing various alloying elements (like Dy, Pr, Al, Cu, Co, etc.) in addition to Nd, Fe, and B. Very seldom, the data points were above the line for three-component Nd-Fe-B alloys. If the portion of completely wetted Nd₂Fe₁₄B/Nd₂Fe₁₄B GBs is so low and the amount of wetting phase is high, what is the mechanism for the formation of magnetically isolating Nd-rich layers between Nd₂Fe₁₄B grains which are needed for high performance of the NdFeB-based alloys for permanent magnets? Can the pseudopartial GB wetting be the explanation?

If one observes the thin GB layers of a constant thickness (or complexions), it is not easy to distinguish whether one has the case of (1) prewetting/prewetting in the one-phase area of a bulk phase diagram; (2) thin GB “pancake” due to the deficit of wetting phase; or (3) pseudopartial wetting by a liquid or solid phase. The big problem is that most frequently the bulk liquid or solid phase can be found only in the GB TJ “pockets.” The pseudopartial wetting can be clearly identified only if the contact angle $\theta \geq 60^\circ$ and the solid/liquid interface

is convex (Fig. 2a, b). If the contact angle $\theta < 60^\circ$ and the solid/liquid interface is concave (Fig. 2c, d), the difference becomes very fine. If the solid/liquid interface has a discontinuity (two tangentials) between TJ pocket and GB layer (Fig. 2c), the pseudopartial wetting takes place. If the solid/liquid interface is continuous (one tangential) between TJ pocket and GB layer (Fig. 2d), the complete wetting with the deficit of wetting phase takes place.

Can the $\text{Nd}_2\text{Fe}_{14}\text{B}/\text{Nd}_2\text{Fe}_{14}\text{B}$ GBs contain the few-nanometer-thick Nd-rich layers like the prewetting GB layers in metals (Ref 17–22, 42, 56–62) or oxides (Ref 5–16)? Already in early 1990s, such few-nm-thin Nd-rich GB layers were indeed observed in the NdFeB-based alloys (Ref 63). Later, the Nd-rich uniformly thick layers between $\text{Nd}_2\text{Fe}_{14}\text{B}$ grains with thickness below 5 nm were observed in various alloys in many experimental works (Ref 63–76). What is the physical reason for the formation of such uniformly thick GB layers of few nanometer thickness? As we saw above, two possibilities exist for the explanation of this phenomenon. First one is the complete GB wetting by a liquid phase in case of a deficit of a melt. In this case, the liquid pockets in the GB TJs could still completely wet the TJs and form the continuous network along TJs. The TJ pockets make then the impression that the amount of a liquid phase is not as low. Nevertheless, the liquid phase distributes in this case in such a way that the pockets in TJs remain macroscopic (i.e., few μm in diameter), but in GBs the melt is in a deficit and is able to cover the GBs only with a few-nm-thin films. In this case, the liquid in the TG pocket should undergo into a thin GB layer without any shape discontinuity (like it is shown in the scheme in Fig. 2c). Such continuous shape transition between TJ pocket and GB film has been indeed observed in various experiments (Ref 53, 65, 66, 77–80). In numerous papers, one can see in the published micrographs simultaneously TJs with (solidified by cooling) liquid inside and thin film in GBs (Ref 53, 63, 65–67, 76–81).

Second possible explanation for the existence of the uniformly thin GB layers is the pseudopartial GB wetting (like it is shown in the scheme in Fig. 2a, b, c). In this case, there should be a shape discontinuity (break of the first shape derivative) in the contact point between liquid TJ pocket and thin GB layer. It is easy to judge about pseudopartial GB wetting if the contact angle is equal or above 60° (like in Fig. 2a and b). If the contact angle is small (like it is shown in Fig. 2c), the transition between liquid in TJ and (quasi)liquid in GB is rather smooth, and the discontinuity is weak and not easy to distinguish from the case of complete wetting and deficit of a melt (Fig. 2d) like in Fig. 7b from the Ref 53. On the other hand, in many papers the TEM micrographs were published where the pseudopartial GB wetting most probably takes place (Ref 63, 66, 67, 73, 76, 78, 79, 81). In any case, in order to conclude about the nature of thin GB layers one needs the micrographs where both TJ pockets and GB layers are visible. Unfortunately, in the majority of cases the published micrographs of thin Nd-rich GB layers do not contain the places where the GB contacts with an Nd-rich pocket in a TJ. In such cases, it is not easy or even not possible to judge, whether we deal with complete GB wetting with deficit of wetting phase or pseudopartial GB wetting.

The results obtained in our work show without any doubt that the NdFeB-based alloys, together with few completely wetted GBs, can contain GBs either incompletely or pseudo-incompletely wetted by the Nd-rich melt. In first case (GBs A and B in Fig. 3a), the GBs remain “dry” and are not enriched (depleted)

by the Fe and/or Nd (Fig. 3d and e). The GBs A and B also have the non-zero contact angle with Nd-rich phase in the TJ. Therefore, the GBs A and B are incompletely wetted by the Nd-rich melt. This situation corresponds to the scheme shown in Fig. 1b. The pseudo-incompletely (or pseudopartially) wetted GB C also has the non-zero contact angle with Nd-rich phase in the TJ (similar to the GBs A and B). However, the GB C contains the thin layer which is enriched by Nd and depleted by Fe (Fig. 3f). This layer is uniformly thin (about 5 nm) and also clearly visible in TEM and HREM micrographs (Fig. 3b and c). Since GB C is not “dry” and contains the thin Nd-rich layer, this situation corresponds to the scheme shown in Fig. 1f and 2c. In other words, the GB C is pseudo-incompletely (or pseudopartially) wetted by the Nd-rich melt.

The completely, incompletely, and pseudopartially wetted $\text{Nd}_2\text{Fe}_{14}\text{B}/\text{Nd}_2\text{Fe}_{14}\text{B}$ GBs as well their TJs (filled by the Nd-rich melt) form the continuous network with a complicated topology. The contiguity of this network defined the ability of $\text{Nd}_2\text{Fe}_{14}\text{B}/\text{Nd}_2\text{Fe}_{14}\text{B}$ GBs to fix the magnetic domain walls and to prevent its movement. Such magnetic isolation increases the magnetic energy product HB of NdFeB-based hard magnetic alloys.

5. Conclusions

In this work, we observed for the first time that the boundaries between grains of $\text{Nd}_2\text{Fe}_{14}\text{B}$ hard magnetic phase in the NdFeB-based permanent magnets can be pseudo-incompletely (or pseudopartially) wetted by the Nd-rich melt. Such GBs form the non-zero contact angle with the melt in the TJs and, simultaneously, contain the uniformly thin (about 5 nm) Nd-rich layer. Therefore, they are different from the completely wetted GBs (zero contact angle and non-uniform and thick Nd-rich layer with thickness above 100 nm) and incompletely wetted GBs (non-zero contact angle, no Nd-rich layer). The thin Nd-rich layers in the pseudo-incompletely (pseudopartially) wetted $\text{Nd}_2\text{Fe}_{14}\text{B}/\text{Nd}_2\text{Fe}_{14}\text{B}$ GBs are most probably responsible for the excellent magnetic properties of the NdFeB-based permanent magnets. It is because these layers can ensure the magnetic isolation between the $\text{Nd}_2\text{Fe}_{14}\text{B}$ grains needed for the high coercivity.

Acknowledgments

This work was performed under the partial financial support of Russian Foundation for Basic Research (Grants 14-42-03621, 15-03-01127, and 15-53-06008), Israeli Ministry of Science, Technology and Space, and Karlsruhe Nano Micro Facility operated by the by the Karlsruhe Institute of Technology.

References

1. B.B. Straumal, A.A. Mazilkin, S.G. Protasova, A.A. Myatiev, P.B. Straumal, G. Schütz, P.A. van Aken, E. Goering, and B. Baretzky, Grain-Boundary Induced High T_c -Ferromagnetism in Pure and Doped Nanocrystalline ZnO, *Phys. Rev. B*, 2009, **79**, p 205206
2. B. Zhao, G. Gottstein, and L.S. Shvindlerman, Triple Junction Effects in Solids, *Acta Mater.*, 2011, **59**, p 3510–3518
3. J.G. Dash, H. Fu, and J.S. Wettlaufer, The Premelting of Ice and Its Environmental Consequences, *Rep. Prog. Phys.*, 1995, **58**, p 115–167
4. P. Bueno, J. Varela, and E. Longo, SnO_2 , ZnO and Related Polycrystalline Compound Semiconductors, An Overview and Review

- on the Voltage-Dependent Resistance (Non-Ohmic) Feature, *J. Eur. Ceram. Soc.*, 2008, **28**, p 505–529
5. J. Luo, Y.M. Chiang, and R.M. Cannon, Nanometer-Thick Surficial Films in Oxides as a Case of Prewetting, *Langmuir*, 2005, **21**, p 7358–7365
 6. J. Luo, M. Tang, R.M. Cannon, W.C. Carter, and Y.M. Chiang, Pressure-Balance and Diffuse-Interface Models for Surficial Amorphous Films, *Mater. Sci. Eng. A*, 2006, **422**, p 19–28
 7. D.R. Clarke, On the Equilibrium Thickness of Intergranular Glass Phases in Ceramic Materials, *J. Am. Ceram. Soc.*, 1987, **70**, p 15–22
 8. J. Luo, Stabilization of Nanoscale Quasi-Liquid Interfacial Films in Inorganic Materials: A Review and Critical Assessment, *Crit. Rev. Solid State Mater. Sci.*, 2007, **32**, p 67–109
 9. J. Luo and Y.M. Chiang, Wetting and Prewetting on Ceramic Surfaces, *Ann. Rev. Mater. Res.*, 2008, **38**, p 227–249
 10. A. Subramaniam, C. Koch, R.M. Cannon, and M. Rühle, Intergranular Glassy Films: An Overview, *Mater. Sci. Eng. A*, 2006, **422**, p 3–18
 11. I. Maclaren, Imaging and Thickness Measurement of Amorphous Intergranular Films Using TEM, *Ultramicroscopy*, 2004, **99**, p 103–113
 12. S.J. Dillon, M. Tang, W. Craig Carter, and M.P. Harmer, Complexion: A New Concept for Kinetic Engineering in Materials Science, *Acta Mater.*, 2007, **55**, p 6208–6218
 13. M.P. Harmer, Interfacial Kinetic Engineering: How Far Have We Come Since Kingery's Inaugural Sosman Address?, *J. Am. Ceram. Soc.*, 2010, **93**, p 301–317
 14. S.G. Protasova, B.B. Straumal, A.A. Mazilkin, S.V. Stakhanova, P.B. Straumal, and B. Baretzky, Increase of Fe Solubility in ZnO Induced by the Grain Boundary Adsorption, *J. Mater. Sci.*, 2014, **49**, p 4490–4498
 15. Th Tietze, P. Audehm, Y.C. Chen, G. Schütz, B.B. Straumal, S.G. Protasova, A.A. Mazilkin, P.B. Straumal, Th Prokscha, H. Luetkens, Z. Salman, A. Suter, B. Baretzky, K. Fink, W. Wenzel, D. Danilov, and E. Goering, Interfacial Dominated Ferromagnetism in Nanograined ZnO: A μ SR and DFT Study, *Sci. Rep.*, 2015, **5**, p 8871
 16. B.B. Straumal, A.A. Mazilkin, S.G. Protasova, S.V. Stakhanova, P.B. Straumal, M.F. Bulatov, G. Schütz, Th Tietze, E. Goering, and B. Baretzky, Grain Boundaries as a Source of Ferromagnetism and Increased Solubility of Ni in Nanograined ZnO, *Rev. Adv. Mater. Sci.*, 2015, **41**, p 61–71
 17. B. Straumal, R. Valiev, O. Kogtenkova, P. Zieba, T. Czeppe, E. Bielanska, and M. Faryna, Thermal Evolution and Grain Boundary Phase Transformations in Severe Deformed Nanograined Al-Zn Alloys, *Acta Mater.*, 2008, **56**, p 6123–6131
 18. O.A. Kogtenkova, B.B. Straumal, S.G. Protasova, A.S. Gornakova, P. Zięba, and T. Czeppe, Effect of the Wetting of Grain Boundaries on the Formation of a Solid Solution in the Al-Zn System, *JETP Lett.*, 2012, **96**, p 380–384
 19. R.Z. Valiev, MYu Murashkin, and B.B. Straumal, Enhanced Ductility in Ultrafine-Grained Al Alloys Produced by SPD Techniques, *Mater. Sci. Forum*, 2009, **633–634**, p 321–332
 20. R.Z. Valiev, M.Y. Murashkin, A. Kilmametov, B.B. Straumal, N.Q. Chinh, and T.G. Langdon, Unusual Super-Ductility at Room Temperature in an Ultrafine-Grained Aluminum Alloy, *J. Mater. Sci.*, 2010, **45**, p 4718–4724
 21. N.Q. Chinh, T. Csanádi, J. Gubicza, R.Z. Valiev, B.B. Straumal, and T.G. Langdon, The Effect of Grain-Boundary Sliding and Strain Rate Sensitivity on the Ductility of Ultrafine-Grained Materials, *Mater. Sci. Forum*, 2011, **667–669**, p 677–682
 22. N.Q. Chinh, T. Csanádi, T. Györi, R.Z. Valiev, B.B. Straumal, M. Kawasaki, and T.G. Langdon, Strain Rate Sensitivity Studies in an Ultrafine-Grained Al-30 wt.% Zn Alloy Using Micro- and Nanoindentation, *Mater. Sci. Eng. A*, 2012, **543**, p 117–120
 23. S. Rafäi, D. Bonn, E. Bertrand, and J. Meunier, Long-Range Critical Wetting, Observation of a Critical End Point, *Phys. Rev. Lett.*, 2004, **92**, p 245701
 24. B.B. Straumal, X. Sauvage, B. Baretzky, A.A. Mazilkin, and R.Z. Valiev, Grain Boundary Films in Al-Zn Alloys after High Pressure Torsion, *Scripta Mater.*, 2014, **70**, p 59–62
 25. B.B. Straumal, A.A. Mazilkin, X. Sauvage, R.Z. Valiev, A.B. Straumal, and A.M. Gusak, Pseudopartial Wetting of Grain Boundaries in Severely Deformed Al-Zn Alloys, *Russ. J. Non-Ferrous Met.*, 2015, **56**, p 44–51
 26. B.B. Straumal, I. Konyashin, B. Ries, A.B. Straumal, A.A. Mazilkin, K.I. Kolesnikova, A.M. Gusak, and B. Baretzky, Pseudopartial Wetting of WC/WC Grain Boundaries in Cemented Carbides, *Mater. Lett.*, 2015, **147**, p 105–108
 27. J.W. Cahn, Critical Point Wetting, *J. Chem. Phys.*, 1977, **66**, p 3667–3676
 28. C. Ebner and W.F. Saam, New Phase-Transition Phenomena in Thin Argon Films, *Phys. Rev. Lett.*, 1977, **38**, p 1486–1489
 29. B.B. Straumal, L.M. Klinger, and L.S. Shvindlerman, The Effect of Crystallographic Parameters of Interphase Boundaries on Their Surface Tension and Parameters of the Boundary Diffusion, *Acta Metall.*, 1984, **32**, p 1355–1364
 30. B.B. Straumal, S.A. Polyakov, and E.J. Mittemeijer, Temperature Influence on the Faceting of $\Sigma 3$ and $\Sigma 9$ Grain Boundaries in Cu, *Acta Mater.*, 2006, **54**, p 167–172
 31. J. Schöhlhammer, B. Baretzky, W. Gust, E. Mittemeijer, and B. Straumal, Grain Boundary Grooving as an Indicator of Grain Boundary Phase Transformations, *Interface Sci.*, 2001, **9**, p 43–53
 32. B. Straumal, T. Muschik, W. Gust, and B. Predel, The Wetting Transition in High and Low Energy Grain Boundaries in the Cu(In) System, *Acta Metal. Mater.*, 1992, **40**, p 939–945
 33. B. Straumal, G. López, W. Gust, and E. Mittemeijer, *Nanomaterials by Severe Plastic Deformation. Fundamentals—Processing—Applications*, M.J. Zehetbauer and R.Z. Valiev, Ed., Wiley VCH, Weinheim, 2004, p 642–647
 34. C.-H. Yeh, L.-S. Chang, and B.B. Straumal, The Study on the Solidus Line in Sn-rich Region of Sn-In Phase Diagram, *J. Phase Equilibria Diff.*, 2009, **30**, p 254–257
 35. B.B. Straumal, G. López, E.J. Mittemeijer, W. Gust, and A.P. Zhilyaev, Grain Boundary Phase Transitions in the Al-Mg System and Their Influence on the High-Strain Rate Superplasticity, *Def. Diff. Forum*, 2003, **216–217**, p 307–312
 36. B.B. Straumal, A.S. Gornakova, O.A. Kogtenkova, S.G. Protasova, V.G. Sursaeva, and B. Baretzky, Continuous and Discontinuous Grain Boundary Wetting in the Zn-Al System, *Phys. Rev. B*, 2008, **78**, p 054202
 37. V. Murashov, B. Straumal, and P. Protsenko, Grain Boundary Wetting in Zn Bicrystals by a Sn-Based Melt, *Def. Diff. Forum*, 2006, **249**, p 235–238
 38. C.-H. Yeh, L.-S. Chang, and B.B. Straumal, The Grain Boundary Wetting in the Sn–25 at.% In Alloys, *Def. Diff. Forum*, 2006, **258–260**, p 491–496
 39. B. Straumal, D. Molodov, and W. Gust, Wetting Transition on the Grain Boundaries in Al Contacting with Sn-Rich Melt, *Interface Sci.*, 1995, **3**, p 127–132
 40. F. Brochard-Wyart, J.M. di Meglio, D. Quéré, and P.G. de Gennes, Spreading of Nonvolatile Liquids in a Continuum Picture, *Langmuir*, 1991, **7**, p 335–338
 41. B.B. Straumal, P. Zieba, and W. Gust, Grain Boundary Phase Transitions and Phase Diagrams, *Int. J. Inorg. Mater.*, 2001, **3**, p 1113–1115
 42. B. Straumal, E. Rabkin, W. Lojkowski, W. Gust, and L.S. Shvindlerman, Pressure Influence on the Grain Boundary Wetting Phase Transition in Fe-Si Alloys, *Acta Mater.*, 1997, **45**, p 1931–1940
 43. E. Bertrand, H. Dobbs, D. Broseta, J. Indekeu, D. Bonn, and J. Meunier, First-order and Critical Wetting of Alkanes on Water, *Phys. Rev. Lett.*, 2000, **85**, p 1282–1285
 44. J. Moon, S. Garoff, P. Wynblatt, and R. Suter, Pseudopartial Wetting and Precursor Film Growth in Immiscible Metal Systems, *Langmuir*, 2004, **20**, p 402–408
 45. N.Q. Chinh, R.Z. Valiev, X. Sauvage, G. Varga, K. Havancsák, M. Kawasaki, B.B. Straumal, and T.G. Langdon, Grain Boundary Phenomena in an Ultrafine-Grained Al-Zn Alloy with Improved Mechanical Behavior for Micro-Devices, *Adv. Eng. Mater.*, 2014, **16**, p 1000–1009
 46. X. Sauvage, M.Y. Murashkin, B.B. Straumal, E. Bobruk, and R.Z. Valiev, Ultrafine Grained Structures Resulting from SPD-Induced Phase Transformation in Al-Zn Alloys, *Adv. Eng. Mater.*, 2015, doi: [10.1002/adem.201500151](https://doi.org/10.1002/adem.201500151)
 47. B.B. Straumal, A.A. Mazilkin, S.G. Protasova, A.M. Gusak, M.F. Bulatov, A.B. Straumal, and B. Baretzky, Grain Boundary Phenomena in NdFeB-Based Hard Magnetic Alloys, *Rev. Adv. Mater. Sci.*, 2014, **38**, p 17–28
 48. Y. Matsuura, Y. Hirotsawa, H. Yamamoto, S. Fujimura, M. Sagawa, and K. Osamura, Phase Diagram of the Nd-Fe-B Ternary System, *Jpn. J. Appl. Phys. Part 2-Lett.*, 1985, **24**, p L635–L637

49. G. Schneider, E.-T. Henig, G. Petzow, and H.H. Stadelmaier, Phase Relations in the System Fe-Nd-B, *Zt. Metallkunde*, 1986, **77**, p 755–761
50. K.G. Knoch, B. Reinsch, and G. Petzow, Nd₂Fe₁₄B—Its Region of Primary Solidification, *Zt. Metallkunde*, 1994, **85**, p 350–353
51. T. Schrell, J. Fidler, and H. Kronmüller, Remanence and Coercivity in Isotropic Nanocrystalline Permanent Magnets, *Phys. Rev. B*, 1994, **49**, p 6100–6110
52. D. Goll, M. Seeger, and H. Kronmüller, Magnetic and Microstructural Properties of Nanocrystalline Exchange Coupled PrFeB Permanent Magnets, *J. Magn. Magn. Mater.*, 1998, **185**, p 49–60
53. N.M. Dempsey, T.G. Woodcock, H. Sepehri-Amin, Y. Zhang, H. Kennedy, D. Givord, K. Hono, and O. Gutfleisch, High-coercivity Nd-Fe-B Thick Films without Heavy Rare Earth Additions, *Acta Mater.*, 2013, **61**, p 4920–4927
54. H. Sepehri-Amin, T. Ohkubo, and K. Hono, The Mechanism of Coercivity Enhancement by the Grain Boundary Diffusion Process of Nd-Fe-B Sintered Magnets, *Acta Mater.*, 2013, **61**, p 1982–1990
55. B.B. Straumal, YuO Kucheev, I.L. Yatskovskaya, I.V. Mogilnikova, G. Schütz, and B. Baretzky, Grain Boundary Wetting in the NdFeB-based Hard Magnetic Alloys, *J. Mater. Sci.*, 2012, **47**, p 8352–8359
56. E.I. Rabkin, V.N. Semenov, L.S. Shvindlerman, and B.B. Straumal, Penetration of Tin and Zinc along Tilt Grain Boundaries 43°[100] in Fe-5at.%Si Alloy: Premelting Phase Transition?, *Acta Metall. Mater.*, 1991, **39**, p 627–639
57. O.I. Noskovich, E.I. Rabkin, V.N. Semenov, B.B. Straumal, and L.S. Shvindlerman, Wetting and Premelting Phase Transitions in 38°[100] Tilt Grain Boundaries in (Fe-12 at.%Si) Zn Alloy in the Vicinity of the A2-B2 Bulk Ordering in Fe-12 at.%Si Alloy, *Acta Metall. Mater.*, 1991, **39**, p 3091–3098
58. B.B. Straumal, O.I. Noskovich, V.N. Semenov, L.S. Shvindlerman, W. Gust, and B. Predel, Premelting Transition on 38° [100] Tilt Grain Boundaries in (Fe-10at.%Si)-Zn Alloys, *Acta Metall. Mater.*, 1992, **40**, p 795–801
59. V.N. Semenov, B.B. Straumal, V.G. Glebovsky, and W. Gust, Preparation of Fe-Si Single Crystals and Bicrystals for Diffusion Experiments by the Electron-Beam Floating Zone Technique, *J. Crystal Growth*, 1995, **151**, p 180–186
60. B. Straumal, E. Rabkin, L. Shvindlerman, and W. Gust, Grain Boundary Zinc Penetration in Fe-Si Alloys: Premelting Phase Transition on the Grain Boundaries, *Mater. Sci. Forum*, 1993, **126–128**, p 391–394
61. V.K. Gupta, D.H. Yoon, H.M. Meyer, and J. Luo, Thin Intergranular Films and Solid-State Activated Sintering in Nickel-Doped Tungsten, *Acta Mater.*, 2007, **55**, p 3131–3142
62. J. Luo, V.K. Gupta, D.H. Yoon, and H.M. Meyer, Segregation-Induced Grain Boundary Premelting in Nickel-Doped Tungsten, *Appl. Phys. Lett.*, 2005, **87**, p 231902
63. L. Li, D.E. Luzzi, and C.D. Graham, High-Resolution Electron-Microscope Study of the Grain boundary Phase in Rapidly Quenched Nd-Fe-B Permanent-Magnet Alloys, *J. Mater. Eng. Perform.*, 1992, **1**, p 205–235
64. N. Watanabe, M. Itakura, and M. Nishida, Microstructure of High Coercivity Nd-Fe-Co-Ga-B Hot-Deformed Magnet Improved by the Dy Diffusion Treatment, *J. Alloys Comp.*, 2013, **557**, p 1–4
65. Y.-G. Park and D. Shindo, Magnetic Domain Structures of Over-quenched Nd-Fe-B Permanent Magnets Studied by Electron Holography, *J. Magn. Magn. Mater.*, 2002, **238**, p 68–74
66. V.V. Volkov and Y. Zhu, Dynamic Magnetization Observations and Reversal Mechanisms of Sintered and Die-Upset Nd-Fe-B Magnets, *J. Magn. Magn. Mater.*, 2000, **214**, p 204–216
67. H. Sepehri-Amin, T. Ohkubo, and K. Hono, Grain Boundary Structure and Chemistry of Dy-diffusion Processed Nd-Fe-B Sintered Magnets, *J. Appl. Phys.*, 2010, **107**, p 09A745
68. K. Hono and H. Sepehri-Amin, Strategy for High-Coercivity Nd-Fe-B Magnets, *Scripta Mater.*, 2012, **67**, p 530–535
69. H. Sepehri-Amin, Y. Ue, T. Ohkubo, K. Hono, and M. Sagawa, Microstructure of Fine-Grained Nd-Fe-B Sintered Magnets with High Coercivity, *Scripta Mater.*, 2011, **65**, p 396–399
70. W.F. Li, H. Sepehri-Amin, T. Ohkubo, N. Hase, and K. Hono, Distribution of Dy in High-Coercivity (Nd, Dy)-Fe-B Sintered Magnet, *Acta Mater.*, 2011, **59**, p 3061–3069
71. H. Sepehri-Amin, T. Ohkubo, T. Nishiuchi, S. Hirotsawa, and K. Hono, Coercivity Enhancement of Hydrogenation-Disproportionation-Desorption-Recombination Processed Nd-Fe-B Powders by the Diffusion of Nd-Cu Eutectic Alloys, *Scripta Mater.*, 2010, **63**, p 1124–1127
72. K. Suresh, T. Ohkubo, Y.K. Takahashi, K. Oh-ishi, R. Gopalan, K. Hono, T. Nishiuchi, N. Nozawa, and S. Hirotsawa, Consolidation of Hydrogenation-Disproportionation-Desorption Recombination Processed Nd-Fe-B Magnets by Spark Plasma Sintering, *J. Magn. Magn. Mater.*, 2009, **321**, p 3681–3686
73. N. Watanabe, H. Umemoto, M. Ishimaru, M. Itakura, M. Nishida, and K. Machida, Microstructure Analysis of Nd-Fe-B Sintered Magnets Improved by Tb-metal Vapour Sorption, *J. Microsc.*, 2009, **236**, p 104–108
74. H. Suzuki, Y. Satsu, and M. Komuro, Magnetic Properties of a Nd-Fe-B Sintered Magnet with Dy Segregation, *J. Appl. Phys.*, 2009, **105**, p 07A734
75. W.F. Li, T. Ohkubo, K. Hono, T. Nishiuchi, and S. Hirotsawa, Coercivity Mechanism of Hydrogenation Disproportionation Desorption Recombination Processed Nd-Fe-B Based Magnets, *Appl. Phys. Lett.*, 2008, **93**, p 052505
76. N. Watanabe, H. Umemoto, M. Itakura, M. Nishida, and K. Machida, Grain Boundary Structure of High Coercivity Nd-Fe-B Sintered Magnets with Tb-Metal Vapor Sorption, *IOP Conf. Series, Mater. Sci. Eng.*, 2009, **1**, p 012033
77. M. Yan, L.Q. Yu, W. Luo, W. Wang, W.Y. Zhang, and Y.H. Wen, Change of Microstructure and Magnetic Properties of Sintered Nd-Fe-B Induced by Annealing, *J. Magn. Magn. Mater.*, 2006, **301**, p 1–5
78. N. Oono, M. Sagawa, R. Kasada, H. Matsui, and A. Kimura, Microstructural Evaluation of Dy-Ni-Al Grain-Boundary-Diffusion (GBD) Treatment on Sintered Nd-Fe-B Magnet, *Mater. Sci. Forum*, 2010, **654**, p 2919–2922
79. Q. Ao, W. Liu, and J. Wu, Microstructure of Explosively Compacted Nd-Fe-B Magnets, *Mater. Trans.*, 2005, **46**, p 123–125
80. Q. Liu, F. Xu, J. Wang, X. Dong, L. Zhang, and J. Yang, An investigation of the Microstructure in the Grain Boundary Region of Nd-Fe-B Sintered Magnet During Post-Sintering Annealing, *Scripta Mater.*, 2013, **68**, p 687–690
81. T.-H. Kim, S.-R. Lee, S. Namkung, and T.-S. Jang, A Study on the Nd-rich Phase Evolution in the Nd-Fe-B Sintered Magnet and its Mechanism During Post-Sintering Annealing, *J. Alloys Comp.*, 2012, **537**, p 261–268